

State-independent experimental test of quantum contextuality in an indivisible system

C. Zu¹, Y.-X. Wang¹, D.-L. Deng^{1,2}, X.-Y. Chang¹, K. Liu¹, P.-Y. Hou¹, H.-X. Yang¹, L.-M. Duan^{1,2}

¹*Center for Quantum Information, IIIS, Tsinghua University, Beijing, China and*

²*Department of Physics, University of Michigan, Ann Arbor, Michigan 48109, USA*

We report the first state-independent experimental test of quantum contextuality on a single photonic qutrit (three-dimensional system), based on a recent theoretical proposal [Yu and Oh, Phys. Rev. Lett. 108, 030402 (2012)]. Our experiment spotlights quantum contextuality in its most basic form, in a way that is independent of either the state or the tensor product structure of the system.

PACS numbers: 03.65.Ta, 42.50.Xa, 03.65.Ca, 03.65.Ud

Contextuality represents a major deviation of quantum theory from classical physics [1, 2]. Non-contextual realism is a pillar of the familiar worldview of classical physics. In a non-contextual world, observables have pre-defined values, which are independent of our choices of measurements. Non-contextuality plays a role also in the derivation of Bell's inequalities, as the property of local realism therein can be seen as a special form of non-contextuality, where the independence of the measurement context is enforced by the no-signalling principle [3–6]. In an attempt to save the non-contextuality of the classical worldview, non-contextual hidden variable theories have been proposed as an alternative to quantum mechanics. In these theories, the outcomes of measurements are associated to hidden variables, which are distributed according to a joint probability distribution. However, the celebrated Kochen-Specker theorem [1–4] showed that non-contextual hidden variable theories are incompatible with the predictions of quantum theory. The original Kochen-Specker theorem is presented in the form of a logical contradiction, which is conceptually striking, but experimentally unfriendly: the presence of unavoidable experimental imperfections motivated a debate on whether or not the non-contextual features highlighted by Kochen-Specker theorem can be actually tested in experiments [7, 8]. As a result of the debate, new Bell-type inequalities have been proposed in the recent years, with the purpose of pinpointing the contextuality of quantum mechanics in an experimentally testable way. These inequalities are generally referred to as the *KS inequalities* [5]. Violation of the KS inequalities confirms quantum contextuality and rules out the non-contextual hidden variable theory. Different from the Bell inequality tests, violation of the KS inequality can be achieved independently of the state of quantum systems [1, 2, 5, 6], showing that the conflict between quantum theory and non-contextual realism resides in the structure of quantum mechanics instead of particular quantum states. The KS inequalities have been tested in experiments for two qubits, using ions [9], photons [10, 11], neutrons [12], or an ensemble nuclear magnetic resonance system [13]. A single qutrit represents

the simplest system where it is possible to observe conflict between quantum theory and non-contextual realistic models [6, 14–16]. A recent experiment has demonstrated quantum contextuality for photonic qutrits in a particular quantum state [14], based on a version of the KS inequality proposed by Klyachko, Can, Binicioglu, and Shumovsky [15].

A state-independent test of quantum contextuality for a single qutrit, in the spirit of the original KS theorem, is possible but complicated as one needs to measure many experimental configurations [4, 6, 16]. A recent theoretical work by Yu and Oh proposes another version of the KS inequality, which requires to measure 13 variables and 24 of their pair correlations [6]. This is a significant simplification compared with the previous KS inequalities for single qutrits, and the number of variables cannot be further reduced as proven recently by Cabello [17]. Our experiment confirms quantum contextuality in a state-independent fashion using the Yu-Oh version of the KS inequality for qutrits represented by three distinctive paths of single photons. The maximum violation of this inequality by quantum mechanics is only 4% beyond the bound set by the non-contextual hidden variable theory, so we need to accurately control the paths of single photons in experiments to measure the 13 variables and their correlations for different types of input states. We have achieved a violation of the KS inequality by more than five standard deviations for all the nine different states that we tested.

For a single qutrit with basis vectors $\{|0\rangle, |1\rangle, |2\rangle\}$, we detect projection operators to the states $i|0\rangle + j|1\rangle + k|2\rangle$ specified by the 13 unit vectors (i, j, k) in Fig. 1. The 13 projectors have eigenvalues either 0 or 1. In the hidden variable theory, the corresponding observables are assigned randomly with values 0 or 1 according to a (generally unknown) joint probability distribution. When two states are orthogonal, the projectors onto them commute, and the corresponding observables are called compatible, which means that they can be measured simultaneously. Non-contextuality means that the assignment of values to an observable should be independent of the choice of compatible observables that are mea-

sured jointly with it. For instance, z_1 in Fig. 1 should be assigned the same value in the correlators $z_1 z_2$ and $z_1 y_1^\pm$ for each trial of measurement. For each observable $b_i \in \{z_\mu, y_\mu^\pm, h_\alpha, \mu = 1, 2, 3; \alpha = 0, 1, 2, 3\}$ defined in Fig. 1, we introduce a new variable $a_i \equiv 1 - 2b_i$, which takes values of ± 1 . For the 13 observables a_i with two outcomes ± 1 , it is shown in Ref. [6] that they satisfy the inequality

$$\sum_i a_i - \frac{1}{4} \sum_{\langle i, j \rangle} a_i a_j \leq 8, \quad (1)$$

where $\langle i, j \rangle$ denotes all pairs of observables that are compatible with each other. There are 24 compatible pairs among all the 13×13 combinations, and a complete list of them is given in Table 1 for the corresponding operator correlations. The inequality (1) can be proven either through an exhaustive check of all the possible 2^{13} value assignments of a_i ($i = 1, 2, \dots, 13$) or by a more elegant analytic argument as shown in Ref. [6]. In quantum theory, each a_i corresponds to an operator A_i with eigenvalues ± 1 in quantum mechanics. In the hidden variable theory, the value a_i corresponds to a random variable A_i , and the different values are distributed according to a (possibly correlated) joint probability distribution. Hence, for the hidden variable theory the expectation values of A_i must satisfy the inequality

$$\sum_i \langle A_i \rangle - \frac{1}{4} \sum_{\langle i, j \rangle} \langle A_i A_j \rangle \leq 8. \quad (2)$$

which follows by taking the average of (1) over the joint probability distribution of the values a_i . On the other hand, quantum theory gives a different prediction: From the definition $A_i \equiv I - 2B_i$, where B_i is the projection operator to the 13 states in Fig. 1, we find that $S = \sum_i A_i - \frac{1}{4} \sum_{\langle i, j \rangle} A_i A_j \equiv \frac{25}{3}I$, where I is the unity operator. Hence, for any state of the system, quantum theory predicts the inequality $\langle S \rangle = 25/3 \not\leq 8$, which violates the inequality (2) imposed by the non-contextual hidden variable theory and rules out any non-contextual realistic model.

Since the quantum mechanical prediction $\langle S \rangle = 25/3$ is close to the upper bound $\langle S \rangle \leq 8$ set by the non-contextual realism, we need to achieve accurate control in experiments to violate the inequality (2). Yu and Oh also derived another simpler inequality in Ref. [6] by introducing an additional assumption (as proposed in the original KS proof [1, 4]) that the algebraic structure of compatible observables is preserved at the hidden variable level, that is, that the value assigned to the product (or sum) of two compatible observables is equal to the product (or sum) of the values assigned to these observables. Under this assumption, it is shown in [6] that

$$\sum_{\alpha=0,1,2,3} \langle B_{h_\alpha} \rangle \leq 1 \quad (3)$$

for non-contextual hidden variable theory, while quantum mechanically $\sum_{\alpha=0,1,2,3} B_{h_\alpha} \equiv \frac{4}{3}I$, and thus

$$\sum_{\alpha=0,1,2,3} \langle B_{h_\alpha} \rangle = 4/3 > 1. \quad \text{The inequality (3) is more}$$

amenable to experimental tests than Eq. (2), as it requires only four measurement settings. However, conceptually it is weaker than Eq. (2) due to the additional assumption required for its proof. Our experiment achieves significant violation of both the inequalities (2) and (3).

To experimentally test the inequalities (2) and (3), first we prepare a single photonic qutrit through the spontaneous parametric down conversion (SPDC) setup shown in Fig. 2. The SPDC process generates correlated (entangled) photon pairs, and through detection of one of the photons by a detector D0, we get a heralded single-photon source on the other output mode. This photon is then split by two polarizing beam splitters (PBS) into three spatial modes that represent a single photonic qutrit. Through control of the wave plates before the PBS and for the pump light, we can prepare any state for this photonic qutrit.

The state of the qutrit is then detected by three single-photon detectors D1-D3. To measure the observables A_i and their correlations, we use the setup shown in Fig. 1 based on cascaded Mach-Zehnder interferometers. The wave plates HWP3 and HWP4 in the interferometers can be tilted to fine tune the phase difference between the two arms. To stabilize the relative phase, the whole interferometer setup is enclosed in a black box. The detectors D1-D3 measure projections to three orthogonal states in the qutrit space, which always correspond to mutually compatible observables. By tuning the half wave plates HWP5 and HWP6 in Fig. 1, we can choose these projections so that they give a subset of the 13 projection operators B_i . A detector click (non-click) then means assignment of value 1 (0) to the corresponding observable B_i (or equivalently, assignment of -1 ($+1$) to the observable A_i). The coincidence between the detectors measures the correlation. The detailed configurations of the wave plates to measure different correlations are summarized in section 1 of the supplementary information. Due to the photon loss, sometimes our photonic qutrit does not yield a click in the detectors D1-D3, even though we registered a heralding photon at the detector D0. To take this into account, we discard the events when none of the detectors D1-D3 fires, in the same way as it was done in Ref. [14]. The use of this post-selection technique opens up a detection efficiency loophole, and we need to assume that the events selected out by the photonic coincidence is an unbiased representation of the whole sample (*fair-sampling assumption*).

We have measured all the expectation values in the inequality (2) and (3) for different input states. Table 1 summarizes the measurement results for a particular input state $|s\rangle = (|0\rangle + |1\rangle + |2\rangle)/\sqrt{3}$ in equal superpo-

sition of the three basis-vectors. The theoretical values in the quantum mechanical case are calculated using the Born rule with the ideal state $|s\rangle$. Each of the experimental correlations is constructed from the joint probabilities $P(A_i = \pm 1; A_j = \pm 1)$ registered by the detectors. As an example to show the measurement method, in section 2 of the supplementary information, we give detailed data for the registered joint probabilities under different measurement configurations, which together fix all the correlations in Table 1. The expectation value $\langle B_i \rangle$ (or $\langle A_i \rangle \equiv 1 - 2\langle B_i \rangle$) is directly determined by the relative probability of the photon firing in the corresponding detector. From the data summarized in Table 1, we find both of the inequalities (2) and (3) are significantly violated in experiments, in agreement with the quantum mechanics prediction and in contradiction with the non-contextual realistic models. Even the tough inequality (2) is violated by more than five times the error bar (standard deviation).

To verify that the inequalities (2) and (3) are experimentally violated independently of the state of the system, we have tested them for different kinds of input states. The set of states tested include the three basis-vectors $\{|0\rangle, |1\rangle, |2\rangle\}$, the two-component superposition states $\{(|0\rangle + |1\rangle)/\sqrt{2}, (|0\rangle + |2\rangle)/\sqrt{2}, (|1\rangle + |2\rangle)/\sqrt{2}\}$, the three-component superposition state $|s\rangle$, and two mixed states $\rho_8 = (|0\rangle\langle 0| + |2\rangle\langle 2|)/2$ and $\rho_9 = (|0\rangle\langle 0| + |1\rangle\langle 1| + |2\rangle\langle 2|)/3 \equiv I/3$. The detailed configurations of the wave plates to prepare these different input states are summarized in section 1 of the supplementary information. To generate the mixed states, we first produce photon pairs entangled in polarization using the type-I phase matching in the BBO crystal [18]. After tracing out the idler photon by the detection at D0, we get a mixed state in polarization for the signal photon, which is then transferred to a mixed qutrit state represented by the optical paths through the PBS. For various input states, we measure correlations of all the observables in the inequality (2) and the detailed results are presented in section 3 of the supplementary information. Although the expectation values $\langle A_i \rangle$ and the correlations $\langle A_i A_j \rangle$ strongly depend on the input states, the inequalities (2) and (3) are state-independent and significantly violated for all the cases tested in experiments. In Fig. 3, we present the measurement outcomes of these two inequalities for nine different input states. The results violate the boundary set by the non-contextual hidden variable theory and are in excellent agreement with quantum mechanics predictions.

In this work, we have observed violation of the KS inequalities (2) and (3) for a single photonic qutrit, which represents the first state-independent experimental test of quantum contextuality in an indivisible quantum system. The experiment confirmation of quantum contex-

tuality in its most basic form, in a way that is independent of either the state or the tensor product structure of

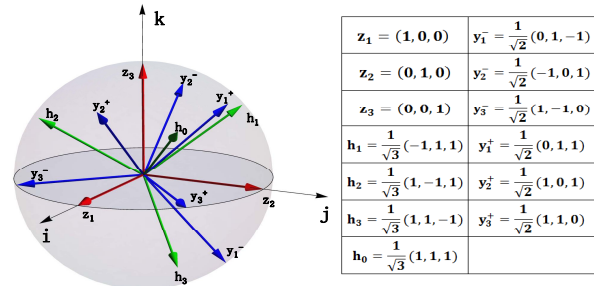


FIG. 1: Illustration of the 13 unit-vectors that describe the superposition coefficients of 13 corresponding qutrit states. The KS inequality proposed in Ref. [6] requires to detect projection operators onto these 13 states and their correlations.

the system, sheds new light on the contradiction between quantum mechanics and non-contextual realistic models.

Acknowledgement This work was supported by the National Basic Research Program of China (973 Program) 2011CBA00300 (2011CBA00302) and the NSFC Grant 61033001. DLD and LMD acknowledge in addition support from the IARPA MUSIQC program, the ARO and the AFOSR MURI program.

-
- [1] S. Kochen and E. P. Specker, J. Math. Mech. 17, 59 (1967).
 - [2] J. S. Bell, Rev. Mod. Phys. 38, 447 (1966).
 - [3] N. D. Mermin, Phys. Rev. Lett. 65, 3373 (1990).
 - [4] A. Peres, Quantum Theory: Concepts and Methods Ch. 7 (Kluwer, 1993).
 - [5] A. Cabello, Phys. Rev. Lett. 101, 210401 (2008).
 - [6] S. X. Yu and C. H. Oh, Phys. Rev. Lett. 108, 030402-1-5 (2012).
 - [7] D. A. Meyer, Phys. Rev. Lett. 83, 3751 (1999).
 - [8] A. Kent, Phys. Rev. Lett. 83, 3755 (1999).
 - [9] G. Kirchmair et al. Nature 460, 494 (2009).
 - [10] E. Amsalem, M. Radmark, M. Bourennane, A. Cabello, Phys. Rev. Lett. 103, 160405 (2009).
 - [11] Y.-F. Huang et al., Phys. Rev. Lett. 90, 250401 (2003).
 - [12] H. Bartosik et al., Phys. Rev. Lett. 103, 040403 (2009).
 - [13] O. Moussa, C. A. Ryan, D. G. Cory, R. Laflamme, Phys. Rev. Lett. 104, 160501 (2010).
 - [14] R. Lapkiewicz et al., Nature (London) 474, 490 (2011).
 - [15] A. A. Klyachko, M. A. Can, S. Binicioglu, A. S. Shumovsky, Phys. Rev. Lett. 101, 20403 (2008).
 - [16] P. Badziag, I. Bengtsson, A. Cabello, and I. Pitowsky, Phys. Rev. Lett. 103, 050401 (2009).
 - [17] A. Cabello, Preprint: arXiv:1112.5149.
 - [18] P. G. Kwiat, E. Waks, A. G. White, I. Appelbaum, Phys. Rev. A 60, R773 (1999).

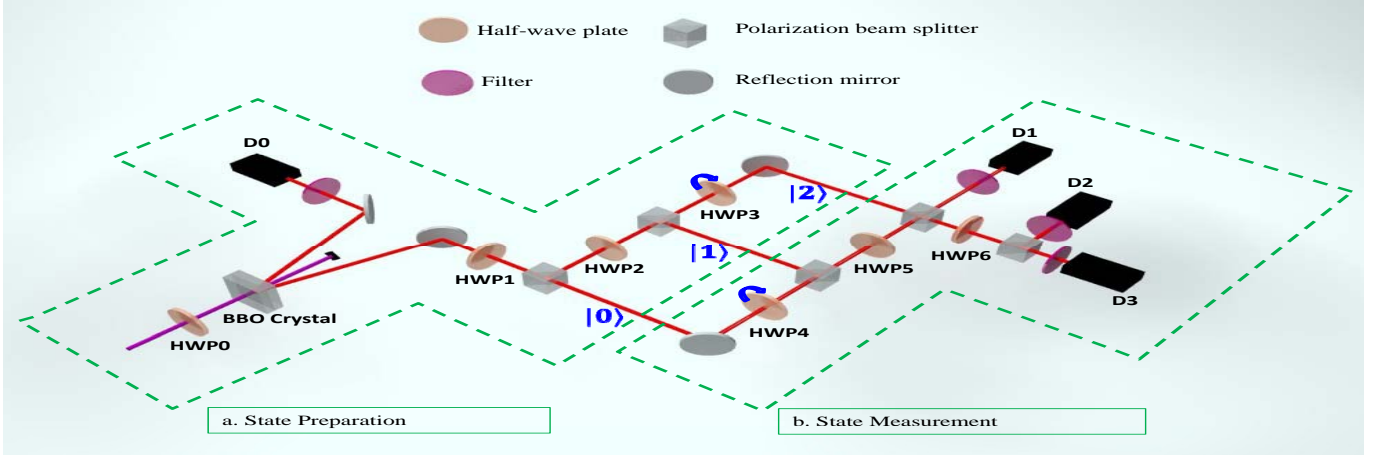


FIG. 2: Illustration of the experimental setup to detect the KS inequalities. The setup in the box (a) is for state preparation of a single photonic qutrit. Ultrafast laser pulses (with a repetition rate of 76 MHz) at the wavelength of 400 nm from a frequency doubled Ti:sapphire laser pump two joint beta-barium-borate (BBO) crystals, each of 0.6 mm depth with perpendicular optical axis, to generate correlated (entangled) photon pairs at the wavelength of 800 nm. With registration of a photon-count at the detector D0, we get a heralded single photon source in the other output mode. This photon is split by two polarizing beam splitters (PBS) into three optical paths, representing a single photonic qutrit. By adjusting the angle of the half wave plates (HWP1 and HWP2), we can control the superposition coefficients of this qutrit state. The setup in box (b) is for measurement of the qutrit state along compatible projections to three orthogonal states. By tuning the wave plates (HWP5 and HWP6), we choose these projection operators to be along the directions specified by the A_i operators to measure the correlations of the compatible A_i . The wave plates HWP3 and HWP4 are used to balance the Mach-Zender interferometers and can be tilted for fine tuning of the relative phase.

Observables	Experimental value	Theoretical prediction	Observables	Experimental value	Theoretical prediction	Observables	Experimental value	Theoretical prediction
$\langle A_{z_1} \rangle$	0.328(18)	0.333	$\langle A_{z_1} A_{z_2} \rangle$	-0.348(18)	-0.333	$\langle A_{y_1^+} A_{h_2} \rangle$	-0.628(17)	-0.555
$\langle A_{z_2} \rangle$	0.324(18)	0.333	$\langle A_{z_2} A_{z_3} \rangle$	-0.324(18)	-0.333	$\langle A_{y_1^+} A_{h_3} \rangle$	-0.481(16)	-0.555
$\langle A_{z_3} \rangle$	0.348(18)	0.333	$\langle A_{z_1} A_{z_3} \rangle$	-0.328(18)	-0.333	$\langle A_{y_2^-} A_{y_3^+} \rangle$	-0.317(17)	-0.333
$\langle A_{y_1^+} \rangle$	-0.320(17)	-0.333	$\langle A_{z_1} A_{y_1^+} \rangle$	-0.876(9)	-1	$\langle A_{y_2^-} A_{h_0} \rangle$	-0.940(6)	-1
$\langle A_{y_1^-} \rangle$	0.876(9)	1	$\langle A_{z_1} A_{y_1^-} \rangle$	0.320(17)	0.333	$\langle A_{y_2^+} A_{h_1} \rangle$	-0.435(16)	-0.555
$\langle A_{y_2^+} \rangle$	-0.220(17)	-0.333	$\langle A_{z_2} A_{y_2^+} \rangle$	-0.903(8)	-1	$\langle A_{y_2^-} A_{h_2} \rangle$	0.682(13)	0.778
$\langle A_{y_2^-} \rangle$	0.903(8)	1	$\langle A_{z_2} A_{y_2^-} \rangle$	0.220(17)	0.333	$\langle A_{y_3^+} A_{h_3} \rangle$	-0.572(15)	-0.555
$\langle A_{y_3^+} \rangle$	-0.255(18)	-0.333	$\langle A_{z_3} A_{y_3^+} \rangle$	-0.939(6)	-1	$\langle A_{y_3^-} A_{y_1^+} \rangle$	-0.315(18)	-0.333
$\langle A_{y_3^-} \rangle$	0.939(6)	1	$\langle A_{z_3} A_{y_3^-} \rangle$	0.255(18)	0.333	$\langle A_{y_3^-} A_{h_0} \rangle$	-0.979(4)	-1
$\langle A_{h_0} \rangle$	-0.943(6)	-1	$\langle A_{y_1^-} A_{y_2^+} \rangle$	-0.444(17)	-0.333	$\langle A_{y_3^+} A_{h_1} \rangle$	-0.480(16)	-0.555
$\langle A_{h_1} \rangle$	0.745(12)	0.778	$\langle A_{y_1^-} A_{h_0} \rangle$	-0.938(6)	-1	$\langle A_{y_3^+} A_{h_2} \rangle$	-0.510(16)	-0.555
$\langle A_{h_2} \rangle$	0.817(10)	0.778	$\langle A_{y_1^-} A_{h_1} \rangle$	0.698(12)	0.778	$\langle A_{y_3^-} A_{h_3} \rangle$	0.710(13)	0.778
$\langle A_{h_3} \rangle$	0.746(12)	0.778						
K-S Inequality (2)		$\sum_i \langle A_i \rangle - \frac{1}{4} \sum_{(i,j)} \langle A_i A_j \rangle = 8.226 \pm 0.041$			K-S Inequality (3)		$\sum_{\alpha=0,1,2,3} \langle B_{h_\alpha} \rangle = 1.317 \pm 0.011$	

FIG. 3: Table 1: (A) The measured expectation values $\langle A_i \rangle$ and the correlations $\langle A_i A_j \rangle$ for all the compatible pairs under a particular input state $|s\rangle = (|0\rangle + |1\rangle + |2\rangle)/\sqrt{3}$. For the experimental values, the numbers in the bracket represent the statistical error associated with the photon detection under the assumption of a Poissonian distribution for the photon counts, for instance, $\langle A_{z_1} \rangle = 0.328(18) \equiv 0.328 \pm 0.018$. Both of the inequalities (2) and (3) are significantly violated by the experimental data.

SUPPLEMENTARY INFORMATION: STATE-INDEPENDENT EXPERIMENTAL TEST OF QUANTUM CONTEXTUALITY IN AN INDIVISIBLE SYSTEM

This supplementary information gives the detailed configurations and data for the experimental test of state-

independent quantum contextuality on a single photonic qutrit. In Sec. I, we first give the configurations of the wave plates to prepare different input states for a single photonic qutrit, and then summarize the configurations of the experiment to measure all the observables and their

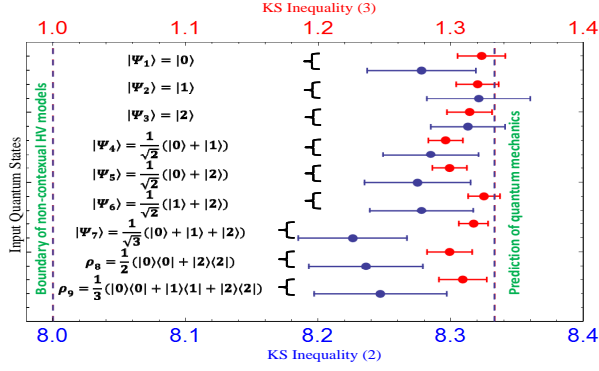


FIG. 4: (A) The measurement results for the two inequalities (2) (shown by the blue label) and (3) (shown by the red label) under different types of input states. The left side dash line specifies the upper bounds imposed by any non-contextual hidden variable models while the right side dash line corresponds to the quantum mechanical prediction under the ideal input states. The error bars account for the statistical error associated with the photon detection.

Input State	HWP0	HWP1	HWP2
$ \Psi_1\rangle = 0\rangle$	0°	0°	0°
$ \Psi_2\rangle = 1\rangle$	0°	45°	0°
$ \Psi_3\rangle = 2\rangle$	0°	45°	-45°
$ \Psi_4\rangle = \frac{1}{\sqrt{2}}(0\rangle + 1\rangle)$	0°	22.5°	0°
$ \Psi_5\rangle = \frac{1}{\sqrt{2}}(0\rangle + 2\rangle)$	0°	22.5°	-45°
$ \Psi_6\rangle = \frac{1}{\sqrt{2}}(1\rangle + 2\rangle)$	0°	45°	-22.5°
$ \Psi_7\rangle = \frac{1}{\sqrt{3}}(0\rangle + 1\rangle + 2\rangle)$	0°	27.37°	-22.5°
$\rho_8 = \frac{1}{2}(0\rangle\langle 0 + 2\rangle\langle 2)$	22.5°	0°	-45°
$\rho_9 = \frac{1}{3}(0\rangle\langle 0 + 1\rangle\langle 1 + 2\rangle\langle 2)$	27.37°	0°	-22.5°

TABLE I: Angles of half-wave plates (HWP) to prepare different states for a single photonic qutrit.

correlations in the KS inequalities. In Sec. II, we show the method to calculate the correlations from the measured joint probabilities, using a particular input state as an example. In Sec. III, we give the detailed data of the correlation measurements for the other eight input states that are not present in the main manuscript.

CONFIGURATIONS OF THE WAVE PLATES FOR STATE PREPARATION AND MEASUREMENT

To demonstrate that the violation of the KS inequalities is independent of the state of the system, we need to prepare different types of input states for the single photonic qutrit. This is achieved by adjusting the

angles of three half wave plates HWP0, HWP1, and HWP2 in the experimental setup shown in Fig. 2 of the manuscript. To prepare pure input state, the polarization of the pumping laser is set to $|V\rangle$ (vertically polarized) by the HWP0. With the type-I phase matching in the BBO nonlinear crystal, the generated signal and idler photons are both in the polarization state $|H\rangle$. After the heralding measurement of the idler photon, the polarization of the signal photon is rotated by the HWP1 and HWP2. The polarization beam splitter (PBS) transmits the photon when it is in $|H\rangle$ polarization and reflects it when it is in $|V\rangle$ polarization. The half-wave plate with angle θ transfers the polarization basis-states $|H\rangle$ and $|V\rangle$ by the formula $|H\rangle \rightarrow \cos(2\theta)|H\rangle + \sin(2\theta)|V\rangle$ and $|V\rangle \rightarrow \cos(2\theta)|V\rangle - \sin(2\theta)|H\rangle$. To prepare an arbitrary input state $c_0|0\rangle + c_1|1\rangle + c_2|2\rangle$, the angle of the HWP1 sets the branching ratio $c_0/\sqrt{c_1^2 + c_2^2}$, and the angle of the HWP2 then determines c_1/c_2 . For the seven pure input states in the experiment, the corresponding angles of the HWP1 and HWP2 are listed in Table. I.

It is more striking to see that the KS inequalities are violated even for completely mixed states. To prepare a mixed state for the signal photon, we rotate the polarization of the pumping laser to $(|H\rangle + |V\rangle)/\sqrt{2}$ by setting the angle of HWP0 at 22.5° . The output state for the signal and the idler photon after the BBO crystal is a maximally entangled one with the form $|\Psi\rangle_{si} = (|HH\rangle + e^{i\varphi}|VV\rangle)/\sqrt{2}$, where φ is a relative phase of the two polarization components. After the heralding measurement of the idler photon, the state of the signal photon is described by the reduced density matrix $(|H\rangle\langle H| + |V\rangle\langle V|)/2$. If we set the HWP1 and HWP2 respectively at the angle of 0° and 45° , this polarization mixed state is transferred to the qutrit mixed state $\rho_8 = (|0\rangle\langle 0| + |2\rangle\langle 2|)/2$ as shown in Table 1. To prepare the mixed state ρ_9 (the most noisy qutrit state), we set the HWP0 at the angle 27.37° and the density operator for the signal photon right after the BBO crystal becomes $(|H\rangle\langle H| + 2|V\rangle\langle V|)/3$. When we set the HWP1 and HWP2 respectively at 0° and 22.5° , the photonic qutrit is described by the state $[|0\rangle\langle 0| + |1\rangle\langle 1| + |2\rangle\langle 2| + (e^{i\phi}|1\rangle\langle 2| + H.c.)]/3$, where the relative phase $\phi = 0$ in the ideal case. However, we randomly tilt the HWP3 in this experiment which sets the phase ϕ to a random value. After average over many experimental runs to measure the correlation, the effective state for the qutrit is described by $\rho_9 = (|0\rangle\langle 0| + |1\rangle\langle 1| + |2\rangle\langle 2|)/3 = I/3$, the completely mixed state.

To detect the KS inequalities, we need to measure the 13 observables $\langle A_i \rangle$ and 24 compatible combinations of their pair-wise correlations $\langle A_i A_j \rangle$. By rotating the angles of the HWP5 and HWP6, We choose the measurement bases so that the photon count at the detectors D1, D2, or D3 correspond to a measurement of the compatible combinations of the projection operators A_i . In

HWP5	HWP6	Detector 1	Detector 2	Detector 3
0°	0°	A_{z_1}	A_{z_2}	A_{z_3}
22.5°	0°	$A_{y_3^-}$	$A_{y_3^+}$	A_{z_3}
0°	22.5°	A_{z_1}	$A_{y_1^+}$	$A_{y_1^-}$
45°	22.5°	A_{z_2}	$A_{y_2^+}$	$A_{y_2^-}$
22.5°	17.63°	$A_{y_3^-}$	A_{h_0}	$A_{h_0^c}$
22.5°	-17.63°	$A_{y_3^-}$	A_{h_3}	$A_{h_3^c}$
-22.5°	17.63°	$A_{y_3^+}$	A_{h_1}	$A_{h_1^c}$
67.5°	17.63°	$A_{y_3^+}$	A_{h_2}	$A_{h_2^c}$

TABLE II: Angles of half-wave plates (HWP5 and HWP6 in Fig. 1 of the main manuscript) to measure correlations of different compatible observables, where $A_{h_0^c}$, $A_{h_1^c}$, $A_{h_2^c}$, and $A_{h_3^c}$ correspond, respectively, to the projection operators onto the states $|h_0^c\rangle = (|0\rangle + |1\rangle - 2|2\rangle)/\sqrt{6}$, $|h_1^c\rangle = (-|0\rangle + |1\rangle - 2|2\rangle)/\sqrt{6}$, $|h_2^c\rangle = (|0\rangle - |1\rangle - 2|2\rangle)/\sqrt{6}$, and $|h_3^c\rangle = (|0\rangle + |1\rangle + 2|2\rangle)/\sqrt{6}$.

Table II, we list the angles of the HWP5 and HWP6 and the corresponding operators detected by the single-photon detectors D1, D2, and D3. With these configurations of the wave plates, we read out the 13 expectation values $\langle A_i \rangle$ and 16 of their compatible pair-wise correlations. The other 8 compatible correlations $\langle A_{y_\mu^\pm} A_{h_\alpha} \rangle$ ($\mu = 1, 2; \alpha = 0, 1, 2, 3$) are obtained from the correlations $\langle A_{y_3^\pm} A_{h_\alpha} \rangle$ with an exchange of the basis-vectors $|2\rangle \leftrightarrow |0\rangle$ or $|2\rangle \leftrightarrow |1\rangle$. So, to measure $\langle A_{y_\mu^\pm} A_{h_\alpha} \rangle$, we use the same configurations as specified by the last four rows of Table II and exchange the basis-vectors $|2\rangle \leftrightarrow |0\rangle$ (or $|1\rangle$) in the input state through an appropriate rotation of the HWP1 and HWP2.

CALCULATION OF CORRELATIONS FROM THE MEASURED JOINT PROBABILITIES

The outcomes for observables A_i are either +1 or -1, depending on whether there is a photon click (or no click) in the corresponding photon detector. The correlation $\langle A_i A_j \rangle$ of the compatible observables A_i and A_j

is constructed from the four measured joint probabilities $P(A_i = \pm 1, A_j = \pm 1)$, whereas the latter is read out from coincidence of the single-photon detectors through the relation

$$\begin{aligned} \langle A_i A_j \rangle = & P(A_i = 1, A_j = 1) + P(A_i = -1, A_j = -1) \\ & - P(A_i = 1, A_j = -1) - P(A_i = -1, A_j = 1). \end{aligned} \quad (4)$$

All the events need to be heralded by the single-photon detector D0. So the joint probability $P(A_i = -1, A_j = +1)$ corresponds to the coincidence rate $\langle D0, Di \rangle$ of the detectors D0 and Di, normalized by the total coincidence $\langle D0, D1 \rangle + \langle D0, D2 \rangle + \langle D0, D3 \rangle$. Similar expressions hold for $P(A_i = -1, A_j = 1)$ and $P(A_i = +1, A_j = +1)$. The joint probability $P(A_i = -1, A_j = -1)$ is proportional to the three-photon coincidence rate $\langle D0, Di, Dj \rangle$, which is smaller than the two-photon coincidence rate by about four orders of magnitude in our experiment. So the probability $P(A_i = -1, A_j = -1)$ is significantly less than the error bars for the other joint probabilities and negligible in calculation of the correlation $\langle A_i A_j \rangle$ by Eq. (1).

In table III, we list the measured joint probabilities for all the compatible pairs A_i and A_j , taking the superposition state $|\Psi_7\rangle = |s\rangle = (|0\rangle + |1\rangle + |2\rangle)/\sqrt{3}$ as an example for the input. The corresponding correlations $\langle A_i A_j \rangle$ are calculated using Eq. (1). The number in the bracket represent the error bar on the last (or last two) digits associated with the statistical error in the photon counts.

RESULTS OF CORRELATION MEASUREMENTS AND KS INEQUALITIES FOR OTHER INPUT STATES

In the main manuscript, we have given the measured expectation values $\langle A_i \rangle$ and the correlations $\langle A_i A_j \rangle$ for a particular input state $|\Psi_7\rangle = |s\rangle = (|0\rangle + |1\rangle + |2\rangle)/\sqrt{3}$. We have tested the KS inequalities for 9 different input states, ranging from the simple basis vectors, to the superposition states, and to the most noisy mixed states. For all the input states, we have observed significant violation of the KS inequalities for single photonic qutrits. In this section, we list the measured expectation values $\langle A_i \rangle$ and the correlations $\langle A_i A_j \rangle$ for the other 8 input states (shown in Table IV, V, VI, and VII).

Joint Probability	Value	Joint Probability	Value	Joint Probability	Value	Term	Value
$P(A_{z_1} = 1, A_{z_2} = -1)$	0.338(9)	$P(A_{z_1} = -1, A_{z_2} = 1)$	0.336(9)	$P(A_{z_1} = 1, A_{z_2} = 1)$	0.326(9)	$\langle A_{z_1} A_{z_2} \rangle$	-0.348(18)
$P(A_{z_1} = 1, A_{z_3} = -1)$	0.326(9)	$P(A_{z_1} = -1, A_{z_3} = 1)$	0.336(9)	$P(A_{z_1} = 1, A_{z_3} = 1)$	0.338(9)	$\langle A_{z_1} A_{z_3} \rangle$	-0.324(18)
$P(A_{z_2} = 1, A_{z_3} = -1)$	0.326(9)	$P(A_{z_2} = -1, A_{z_3} = 1)$	0.338(9)	$P(A_{z_2} = 1, A_{z_3} = 1)$	0.336(9)	$\langle A_{z_2} A_{z_3} \rangle$	-0.328(18)
$P(A_{z_1} = 1, A_{y_1^+} = -1)$	0.660(9)	$P(A_{z_1} = -1, A_{y_1^+} = 1)$	0.278(9)	$P(A_{z_1} = 1, A_{y_1^+} = 1)$	0.062(5)	$\langle A_{z_1} A_{y_1^+} \rangle$	-0.876(9)
$P(A_{z_1} = 1, A_{y_1^-} = -1)$	0.062(5)	$P(A_{z_1} = -1, A_{y_1^-} = 1)$	0.278(9)	$P(A_{z_1} = 1, A_{y_1^-} = 1)$	0.660(9)	$\langle A_{z_1} A_{y_1^-} \rangle$	0.320(17)
$P(A_{y_1^-} = 1, A_{y_1^+} = -1)$	0.660(9)	$P(A_{y_1^-} = -1, A_{y_1^+} = 1)$	0.062(5)	$P(A_{y_1^-} = 1, A_{y_1^+} = 1)$	0.278(9)	$\langle A_{y_1^-} A_{y_1^+} \rangle$	-0.444(17)
$P(A_{z_2} = 1, A_{y_2^+} = -1)$	0.610(9)	$P(A_{z_2} = -1, A_{y_2^+} = 1)$	0.341(9)	$P(A_{z_2} = 1, A_{y_2^+} = 1)$	0.048(4)	$\langle A_{z_2} A_{y_2^+} \rangle$	-0.903(8)
$P(A_{z_2} = 1, A_{y_2^-} = -1)$	0.048(4)	$P(A_{z_2} = -1, A_{y_2^-} = 1)$	0.341(9)	$P(A_{z_2} = 1, A_{y_2^-} = 1)$	0.610(9)	$\langle A_{z_2} A_{y_2^-} \rangle$	0.220(17)
$P(A_{y_2^-} = 1, A_{y_2^+} = -1)$	0.610(9)	$P(A_{y_2^-} = -1, A_{y_2^+} = 1)$	0.048(4)	$P(A_{y_2^-} = 1, A_{y_2^+} = 1)$	0.341(9)	$\langle A_{y_2^-} A_{y_2^+} \rangle$	-0.317(17)
$P(A_{z_3} = 1, A_{y_3^+} = -1)$	0.627(9)	$P(A_{z_3} = -1, A_{y_3^+} = 1)$	0.342(9)	$P(A_{z_3} = 1, A_{y_3^+} = 1)$	0.030(5)	$\langle A_{z_3} A_{y_3^+} \rangle$	-0.939(6)
$P(A_{z_3} = 1, A_{y_3^-} = -1)$	0.030(5)	$P(A_{z_3} = -1, A_{y_3^-} = 1)$	0.342(9)	$P(A_{z_3} = 1, A_{y_3^-} = 1)$	0.627(9)	$\langle A_{z_3} A_{y_3^-} \rangle$	0.255(18)
$P(A_{y_3^-} = 1, A_{y_3^+} = -1)$	0.627(9)	$P(A_{y_3^-} = -1, A_{y_3^+} = 1)$	0.030(5)	$P(A_{y_3^-} = 1, A_{y_3^+} = 1)$	0.342(9)	$\langle A_{y_3^-} A_{y_3^+} \rangle$	-0.315(18)
$P(A_{y_1^-} = 1, A_{h_0} = -1)$	0.935(4)	$P(A_{y_1^-} = -1, A_{h_0} = 1)$	0.034(3)	$P(A_{y_1^-} = 1, A_{h_0} = 1)$	0.031(3)	$\langle A_{y_1^-} A_{h_0} \rangle$	-0.938(6)
$P(A_{y_1^-} = 1, A_{h_1} = -1)$	0.111(6)	$P(A_{y_1^-} = -1, A_{h_1} = 1)$	0.040(6)	$P(A_{y_1^-} = 1, A_{h_1} = 1)$	0.849(3)	$\langle A_{y_1^-} A_{h_1} \rangle$	0.698(12)
$P(A_{y_1^+} = 1, A_{h_2} = -1)$	0.132(6)	$P(A_{y_1^+} = -1, A_{h_2} = 1)$	0.682(9)	$P(A_{y_1^+} = 1, A_{h_2} = 1)$	0.186(7)	$\langle A_{y_1^+} A_{h_2} \rangle$	-0.628(17)
$P(A_{y_1^+} = 1, A_{h_3} = -1)$	0.140(6)	$P(A_{y_1^+} = -1, A_{h_3} = 1)$	0.601(9)	$P(A_{y_1^+} = 1, A_{h_3} = 1)$	0.259(8)	$\langle A_{y_1^+} A_{h_3} \rangle$	-0.481(16)
$P(A_{y_2^-} = 1, A_{h_0} = -1)$	0.917(5)	$P(A_{y_2^-} = -1, A_{h_0} = 1)$	0.053(4)	$P(A_{y_2^-} = 1, A_{h_0} = 1)$	0.030(3)	$\langle A_{y_2^-} A_{h_0} \rangle$	-0.940(6)
$P(A_{y_2^+} = 1, A_{h_1} = -1)$	0.133(6)	$P(A_{y_2^+} = -1, A_{h_1} = 1)$	0.585(9)	$P(A_{y_2^+} = 1, A_{h_1} = 1)$	0.283(8)	$\langle A_{y_2^+} A_{h_1} \rangle$	-0.435(16)
$P(A_{y_2^-} = 1, A_{h_2} = -1)$	0.138(6)	$P(A_{y_2^-} = -1, A_{h_2} = 1)$	0.021(3)	$P(A_{y_2^-} = 1, A_{h_2} = 1)$	0.841(7)	$\langle A_{y_2^-} A_{h_2} \rangle$	0.682(13)
$P(A_{y_2^+} = 1, A_{h_3} = -1)$	0.122(6)	$P(A_{y_2^+} = -1, A_{h_3} = 1)$	0.664(8)	$P(A_{y_2^+} = 1, A_{h_3} = 1)$	0.214(7)	$\langle A_{y_2^+} A_{h_3} \rangle$	-0.435(16)
$P(A_{y_3^-} = 1, A_{h_0} = -1)$	0.971(3)	$P(A_{y_3^-} = -1, A_{h_0} = 1)$	0.018(3)	$P(A_{y_3^-} = 1, A_{h_0} = 1)$	0.010(2)	$\langle A_{y_3^-} A_{h_0} \rangle$	-0.979(4)
$P(A_{y_3^+} = 1, A_{h_1} = -1)$	0.128(6)	$P(A_{y_3^+} = -1, A_{h_1} = 1)$	0.613(9)	$P(A_{y_3^+} = 1, A_{h_1} = 1)$	0.260(8)	$\langle A_{y_3^+} A_{h_1} \rangle$	-0.480(16)
$P(A_{y_3^+} = 1, A_{h_2} = -1)$	0.092(5)	$P(A_{y_3^+} = -1, A_{h_2} = 1)$	0.664(8)	$P(A_{y_3^+} = 1, A_{h_2} = 1)$	0.245(8)	$\langle A_{y_3^+} A_{h_2} \rangle$	-0.510(16)
$P(A_{y_3^-} = 1, A_{h_3} = -1)$	0.127(6)	$P(A_{y_3^-} = -1, A_{h_3} = 1)$	0.018(2)	$P(A_{y_3^-} = 1, A_{h_3} = 1)$	0.855(6)	$\langle A_{y_3^-} A_{h_3} \rangle$	0.710(13)

TABLE III: The measured joint probabilities for all the compatible pairs A_i and A_j in the KS inequality under the input state $|\Psi_7\rangle = \frac{1}{\sqrt{3}}(|0\rangle + |1\rangle + |2\rangle)$

Input State $ \Psi_1\rangle = 0\rangle$								
Observables	Experimental value	Theoretical prediction	Observables	Experimental value	Theoretical prediction	Observables	Experimental value	Theoretical prediction
$\langle A_{z_1} \rangle$	-0.996(2)	-1	$\langle A_{z_1} A_{z_2} \rangle$	-0.999(1)	-1	$\langle A_{y_1^+} A_{h_2} \rangle$	0.312(17)	0.333
$\langle A_{z_2} \rangle$	0.997(2)	1	$\langle A_{z_2} A_{z_3} \rangle$	-0.997(2)	-1	$\langle A_{y_1^+} A_{h_3} \rangle$	0.310(16)	0.333
$\langle A_{z_3} \rangle$	0.999(1)	1	$\langle A_{z_1} A_{z_3} \rangle$	0.996(2)	1	$\langle A_{y_2^-} A_{y_2^+} \rangle$	-0.999(1)	-1
$\langle A_{y_1^+} \rangle$	0.999(1)	1	$\langle A_{z_1} A_{y_1^+} \rangle$	-0.999(1)	-1	$\langle A_{y_2^-} A_{h_0} \rangle$	-0.653(15)	-0.667
$\langle A_{y_1^-} \rangle$	0.999(1)	1	$\langle A_{z_1} A_{y_1^-} \rangle$	-0.999(1)	-1	$\langle A_{y_2^+} A_{h_1} \rangle$	-0.642(16)	-0.667
$\langle A_{y_2^+} \rangle$	0.041(21)	0	$\langle A_{z_2} A_{y_2^+} \rangle$	0.040(21)	0	$\langle A_{y_2^-} A_{h_2} \rangle$	-0.651(15)	-0.667
$\langle A_{y_2^-} \rangle$	-0.040(21)	0	$\langle A_{z_2} A_{y_2^-} \rangle$	-0.041(21)	0	$\langle A_{y_2^+} A_{h_3} \rangle$	-0.633(15)	-0.667
$\langle A_{y_3^+} \rangle$	-0.006(21)	0	$\langle A_{z_3} A_{y_3^+} \rangle$	-0.007(21)	0	$\langle A_{y_3^-} A_{y_3^+} \rangle$	-0.999(1)	-1
$\langle A_{y_3^-} \rangle$	0.007(21)	0	$\langle A_{z_3} A_{y_3^-} \rangle$	0.006(21)	0	$\langle A_{y_3^-} A_{h_0} \rangle$	-0.636(15)	-0.667
$\langle A_{h_0} \rangle$	0.331(19)	0.333	$\langle A_{y_1^-} A_{y_1^+} \rangle$	0.998(1)	1	$\langle A_{y_3^+} A_{h_1} \rangle$	-0.676(14)	-0.667
$\langle A_{h_1} \rangle$	0.362(19)	0.333	$\langle A_{y_1^-} A_{h_0} \rangle$	0.339(16)	0.333	$\langle A_{y_3^+} A_{h_2} \rangle$	-0.624(16)	-0.667
$\langle A_{h_2} \rangle$	0.325(18)	0.333	$\langle A_{y_1^-} A_{h_1} \rangle$	0.354(17)	0.333	$\langle A_{y_3^-} A_{h_3} \rangle$	-0.652(15)	-0.667
$\langle A_{h_3} \rangle$	0.335(19)	0.333						
K-S Inequality (2)		$\sum_i \langle A_i \rangle - \frac{1}{4} \sum_{\langle i,j \rangle} \langle A_i A_j \rangle = 8.278 \pm 0.041$			K-S Inequality (3)		$\sum_{\alpha=0,1,2,3} \langle B_{h_\alpha} \rangle = 1.323 \pm 0.018$	

Input State $ \Psi_2\rangle = 1\rangle$								
Observables	Experimental value	Theoretical prediction	Observables	Experimental value	Theoretical prediction	Observables	Experimental value	Theoretical prediction
$\langle A_{z_1} \rangle$	0.999(1)	1	$\langle A_{z_1} A_{z_2} \rangle$	-0.999(1)	-1	$\langle A_{y_1^+} A_{h_2} \rangle$	-0.647(14)	-0.667
$\langle A_{z_2} \rangle$	-0.999(1)	-1	$\langle A_{z_2} A_{z_3} \rangle$	0.999(1)	1	$\langle A_{y_1^+} A_{h_3} \rangle$	-0.649(14)	-0.667
$\langle A_{z_3} \rangle$	0.999(1)	1	$\langle A_{z_1} A_{z_3} \rangle$	-0.999(1)	-1	$\langle A_{y_2^-} A_{y_2^+} \rangle$	0.999(1)	1
$\langle A_{y_1^+} \rangle$	0.023(19)	0	$\langle A_{z_1} A_{y_1^+} \rangle$	0.021(19)	0	$\langle A_{y_2^-} A_{h_0} \rangle$	0.340(17)	0.333
$\langle A_{y_1^-} \rangle$	-0.021(19)	0	$\langle A_{z_1} A_{y_1^-} \rangle$	-0.023(19)	0	$\langle A_{y_2^+} A_{h_1} \rangle$	0.339(16)	0.333
$\langle A_{y_2^+} \rangle$	0.999(1)	1	$\langle A_{z_2} A_{y_2^+} \rangle$	-0.999(1)	-1	$\langle A_{y_2^-} A_{h_2} \rangle$	0.356(16)	0.333
$\langle A_{y_2^-} \rangle$	0.999(1)	1	$\langle A_{z_2} A_{y_2^-} \rangle$	-0.999(1)	-1	$\langle A_{y_2^+} A_{h_3} \rangle$	0.312(16)	0.333
$\langle A_{y_3^+} \rangle$	0.015(17)	0	$\langle A_{z_3} A_{y_3^+} \rangle$	0.014(17)	0	$\langle A_{y_3^-} A_{y_3^+} \rangle$	-0.999(1)	-1
$\langle A_{y_3^-} \rangle$	-0.014(17)	0	$\langle A_{z_3} A_{y_3^-} \rangle$	-0.015(17)	0	$\langle A_{y_3^-} A_{h_0} \rangle$	-0.635(14)	-0.667
$\langle A_{h_0} \rangle$	0.368(16)	0.333	$\langle A_{y_1^-} A_{y_1^+} \rangle$	-0.998(1)	-1	$\langle A_{y_3^+} A_{h_1} \rangle$	-0.666(14)	-0.667
$\langle A_{h_1} \rangle$	0.337(17)	0.333	$\langle A_{y_1^-} A_{h_0} \rangle$	-0.652(13)	-0.667	$\langle A_{y_3^+} A_{h_2} \rangle$	-0.642(14)	-0.667
$\langle A_{h_2} \rangle$	0.354(17)	0.333	$\langle A_{y_1^-} A_{h_1} \rangle$	-0.689(13)	-0.667	$\langle A_{y_3^-} A_{h_3} \rangle$	-0.682(13)	-0.667
$\langle A_{h_3} \rangle$	0.304(18)	0.333						
K-S Inequality (2)		$\sum_i \langle A_i \rangle - \frac{1}{4} \sum_{\langle i,j \rangle} \langle A_i A_j \rangle = 8.321 \pm 0.039$			K-S Inequality (3)		$\sum_{\alpha=0,1,2,3} \langle B_{h_\alpha} \rangle = 1.321 \pm 0.016$	

TABLE IV: The measured expectation values $\langle A_i \rangle$ and the correlations $\langle A_i A_j \rangle$ for all the compatible pairs under input states $|\Psi_1\rangle = |0\rangle$ and $|\Psi_2\rangle = |1\rangle$.

Input State $ \Psi_3\rangle = 2\rangle$								
Observables	Experimental value	Theoretical prediction	Observables	Experimental value	Theoretical prediction	Observables	Experimental value	Theoretical prediction
$\langle A_{z_1} \rangle$	0.999(1)	1	$\langle A_{z_1} A_{z_2} \rangle$	0.983(3)	1	$\langle A_{y_1^+} A_{h_2} \rangle$	-0.624(16)	-0.667
$\langle A_{z_2} \rangle$	0.984(3)	1	$\langle A_{z_2} A_{z_3} \rangle$	-0.984(3)	-1	$\langle A_{y_1^+} A_{h_3} \rangle$	-0.642(16)	-0.667
$\langle A_{z_3} \rangle$	-0.983(3)	-1	$\langle A_{z_1} A_{z_3} \rangle$	-0.999(1)	-1	$\langle A_{y_2^-} A_{y_2^+} \rangle$	-0.984(3)	-1
$\langle A_{y_1^+} \rangle$	-0.009(17)	0	$\langle A_{z_1} A_{y_1^+} \rangle$	-0.020(17)	0	$\langle A_{y_2^-} A_{h_0} \rangle$	-0.637(13)	-0.667
$\langle A_{y_1^-} \rangle$	0.020(17)	0	$\langle A_{z_1} A_{y_1^-} \rangle$	0.009(17)	0	$\langle A_{y_2^+} A_{h_1} \rangle$	-0.666(15)	-0.667
$\langle A_{y_2^+} \rangle$	-0.021(18)	0	$\langle A_{z_2} A_{y_2^+} \rangle$	-0.037(18)	0	$\langle A_{y_2^-} A_{h_2} \rangle$	-0.683(13)	-0.667
$\langle A_{y_2^-} \rangle$	0.037(18)	0	$\langle A_{z_2} A_{y_2^-} \rangle$	0.021(18)	0	$\langle A_{y_2^+} A_{h_3} \rangle$	-0.647(13)	-0.667
$\langle A_{y_3^+} \rangle$	0.982(3)	1	$\langle A_{z_3} A_{y_3^+} \rangle$	-0.999(1)	-1	$\langle A_{y_3^-} A_{y_3^+} \rangle$	0.981(3)	1
$\langle A_{y_3^-} \rangle$	0.999(1)	1	$\langle A_{z_3} A_{y_3^-} \rangle$	-0.982(3)	-1	$\langle A_{y_3^-} A_{h_0} \rangle$	0.326(17)	0.333
$\langle A_{h_0} \rangle$	0.337(17)	0.333	$\langle A_{y_1^-} A_{y_1^+} \rangle$	-0.988(3)	-1	$\langle A_{y_3^+} A_{h_1} \rangle$	0.333(16)	0.333
$\langle A_{h_1} \rangle$	0.349(17)	0.333	$\langle A_{y_1^-} A_{h_0} \rangle$	-0.636(15)	-0.667	$\langle A_{y_3^+} A_{h_2} \rangle$	0.312(17)	0.333
$\langle A_{h_2} \rangle$	0.325(17)	0.333	$\langle A_{y_1^-} A_{h_1} \rangle$	-0.651(15)	-0.667	$\langle A_{y_3^-} A_{h_3} \rangle$	0.352(17)	0.333
$\langle A_{h_3} \rangle$	0.361(16)	0.333						
K-S Inequality (2)		$\sum_i \langle A_i \rangle - \frac{1}{4} \sum_{\langle i,j \rangle} \langle A_i A_j \rangle = 8.313 \pm 0.028$			K-S Inequality (3)		$\sum_{\alpha=0,1,2,3} \langle B_{h_\alpha} \rangle = 1.314 \pm 0.017$	

Input State $ \Psi_4\rangle = \frac{1}{\sqrt{2}}(0\rangle + 1\rangle)$								
Observables	Experimental value	Theoretical prediction	Observables	Experimental value	Theoretical prediction	Observables	Experimental value	Theoretical prediction
$\langle A_{z_1} \rangle$	0.018(18)	0	$\langle A_{z_1} A_{z_2} \rangle$	-0.999(1)	-1	$\langle A_{y_1^+} A_{h_2} \rangle$	0.510(15)	0.5
$\langle A_{z_2} \rangle$	-0.017(18)	0	$\langle A_{z_2} A_{z_3} \rangle$	0.017(18)	0	$\langle A_{y_1^+} A_{h_3} \rangle$	-0.771(11)	-0.833
$\langle A_{z_3} \rangle$	0.999(1)	1	$\langle A_{z_1} A_{z_3} \rangle$	-0.018(18)	0	$\langle A_{y_2^-} A_{y_2^+} \rangle$	-0.027(17)	0
$\langle A_{y_1^+} \rangle$	0.528(15)	0.5	$\langle A_{z_1} A_{y_1^+} \rangle$	-0.497(16)	-0.5	$\langle A_{y_2^-} A_{h_0} \rangle$	-0.736(13)	-0.833
$\langle A_{y_1^-} \rangle$	0.497(16)	0.5	$\langle A_{z_1} A_{y_1^-} \rangle$	-0.528(16)	-0.5	$\langle A_{y_2^+} A_{h_1} \rangle$	0.515(16)	0.5
$\langle A_{y_2^+} \rangle$	0.511(15)	0.5	$\langle A_{z_2} A_{y_2^+} \rangle$	-0.462(15)	-0.5	$\langle A_{y_2^-} A_{h_2} \rangle$	0.514(16)	0.5
$\langle A_{y_2^-} \rangle$	0.462(15)	0.5	$\langle A_{z_2} A_{y_2^-} \rangle$	-0.511(15)	-0.5	$\langle A_{y_2^+} A_{h_3} \rangle$	-0.780(11)	-0.833
$\langle A_{y_3^+} \rangle$	-0.961(5)	-1	$\langle A_{z_3} A_{y_3^+} \rangle$	-0.961(5)	-1	$\langle A_{y_3^-} A_{y_3^+} \rangle$	-1(0)	-1
$\langle A_{y_3^-} \rangle$	0.961(5)	1	$\langle A_{z_3} A_{y_3^-} \rangle$	0.961(5)	1	$\langle A_{y_3^-} A_{h_0} \rangle$	-0.313(15)	-0.333
$\langle A_{h_0} \rangle$	-0.276(17)	-0.333	$\langle A_{y_1^-} A_{y_1^+} \rangle$	0.025(18)	0	$\langle A_{y_3^+} A_{h_1} \rangle$	-0.983(3)	-1
$\langle A_{h_1} \rangle$	0.977(4)	1	$\langle A_{y_1^-} A_{h_0} \rangle$	-0.815(10)	-0.833	$\langle A_{y_3^+} A_{h_2} \rangle$	-0.994(2)	-1
$\langle A_{h_2} \rangle$	0.973(4)	1	$\langle A_{y_1^-} A_{h_1} \rangle$	0.453(15)	0.5	$\langle A_{y_3^-} A_{h_3} \rangle$	-0.359(17)	-0.333
$\langle A_{h_3} \rangle$	-0.267(17)	-0.333						
K-S Inequality (2)		$\sum_i \langle A_i \rangle - \frac{1}{4} \sum_{\langle i,j \rangle} \langle A_i A_j \rangle = 8.285 \pm 0.036$			K-S Inequality (3)		$\sum_{\alpha=0,1,2,3} \langle B_{h_\alpha} \rangle = 1.296 \pm 0.013$	

TABLE V: The measured expectation values $\langle A_i \rangle$ and the correlations $\langle A_i A_j \rangle$ for all the compatible pairs under input states $|\Psi_3\rangle = |2\rangle$ and $|\Psi_4\rangle = (|0\rangle + |1\rangle)/\sqrt{2}$.

Input State $ \Psi_5\rangle = \frac{1}{\sqrt{2}}(0\rangle + 2\rangle)$								
Observables	Experimental value	Theoretical prediction	Observables	Experimental value	Theoretical prediction	Observables	Experimental value	Theoretical prediction
$\langle A_{z_1} \rangle$	0.019(18)	0	$\langle A_{z_1} A_{z_2} \rangle$	0.010(18)	0	$\langle A_{y_1^+} A_{h_2} \rangle$	-0.767(12)	-0.833
$\langle A_{z_2} \rangle$	0.991(2)	1	$\langle A_{z_2} A_{z_3} \rangle$	-0.991(2)	-1	$\langle A_{y_1^+} A_{h_3} \rangle$	0.519(15)	0.5
$\langle A_{z_3} \rangle$	-0.010(18)	0	$\langle A_{z_1} A_{z_3} \rangle$	-0.019(18)	0	$\langle A_{y_2^-} A_{y_2^+} \rangle$	-0.986(15)	-1
$\langle A_{y_1^+} \rangle$	0.520(16)	0.5	$\langle A_{z_1} A_{y_1^+} \rangle$	-0.514(15)	-0.5	$\langle A_{y_2^-} A_{h_0} \rangle$	-0.313(17)	-0.333
$\langle A_{y_1^-} \rangle$	0.514(15)	0.5	$\langle A_{z_1} A_{y_1^-} \rangle$	-0.520(16)	-0.5	$\langle A_{y_2^+} A_{h_1} \rangle$	-0.992(2)	-1
$\langle A_{y_2^+} \rangle$	-0.964(5)	-1	$\langle A_{z_2} A_{y_2^+} \rangle$	-0.978(4)	-1	$\langle A_{y_2^-} A_{h_2} \rangle$	-0.360(17)	-0.333
$\langle A_{y_2^-} \rangle$	0.978(4)	1	$\langle A_{z_2} A_{y_2^-} \rangle$	0.964(5)	1	$\langle A_{y_2^+} A_{h_3} \rangle$	-0.959(5)	-1
$\langle A_{y_3^+} \rangle$	0.503(15)	0.5	$\langle A_{z_3} A_{y_3^+} \rangle$	-0.478(17)	-0.5	$\langle A_{y_3^-} A_{y_3^+} \rangle$	-0.019(18)	0
$\langle A_{y_3^-} \rangle$	0.478(17)	0.5	$\langle A_{z_3} A_{y_3^-} \rangle$	-0.503(15)	-0.5	$\langle A_{y_3^-} A_{h_0} \rangle$	-0.799(11)	-0.833
$\langle A_{h_0} \rangle$	-0.287(17)	-0.333	$\langle A_{y_1^-} A_{y_1^+} \rangle$	0.034(18)	0	$\langle A_{y_3^+} A_{h_1} \rangle$	0.513(16)	0.5
$\langle A_{h_1} \rangle$	0.982(4)	1	$\langle A_{y_1^-} A_{h_0} \rangle$	-0.735(12)	-0.833	$\langle A_{y_3^+} A_{h_2} \rangle$	-0.791(11)	-0.833
$\langle A_{h_2} \rangle$	-0.278(17)	-0.333	$\langle A_{y_1^-} A_{h_1} \rangle$	0.514(16)	0.5	$\langle A_{y_3^-} A_{h_3} \rangle$	0.472(16)	0.5
$\langle A_{h_3} \rangle$	0.981(4)	1						
K-S Inequality (2)		$\sum_i \langle A_i \rangle - \frac{1}{4} \sum_{\langle i,j \rangle} \langle A_i A_j \rangle = 8.275 \pm 0.041$			K-S Inequality (3)		$\sum_{\alpha=0,1,2,3} \langle B_{h_\alpha} \rangle = 1.299 \pm 0.013$	

Input State $ \Psi_6\rangle = \frac{1}{\sqrt{2}}(1\rangle + 2\rangle)$								
Observables	Experimental value	Theoretical prediction	Observables	Experimental value	Theoretical prediction	Observables	Experimental value	Theoretical prediction
$\langle A_{z_1} \rangle$	0.999(1)	1	$\langle A_{z_1} A_{z_2} \rangle$	-0.009(18)	0	$\langle A_{y_1^+} A_{h_2} \rangle$	-0.994(3)	-1
$\langle A_{z_2} \rangle$	-0.008(17)	0	$\langle A_{z_2} A_{z_3} \rangle$	0.008(17)	0	$\langle A_{y_1^+} A_{h_3} \rangle$	-0.983(3)	-1
$\langle A_{z_3} \rangle$	0.009(18)	0	$\langle A_{z_1} A_{z_3} \rangle$	-0.999(1)	-1	$\langle A_{y_2^-} A_{y_2^+} \rangle$	-0.013(18)	0
$\langle A_{y_1^+} \rangle$	-0.963(5)	-1	$\langle A_{z_1} A_{y_1^+} \rangle$	-0.978(4)	-1	$\langle A_{y_2^-} A_{h_0} \rangle$	-0.793(11)	-0.833
$\langle A_{y_1^-} \rangle$	0.978(4)	1	$\langle A_{z_1} A_{y_1^-} \rangle$	0.963(5)	1	$\langle A_{y_2^+} A_{h_1} \rangle$	-0.771(11)	-0.833
$\langle A_{y_2^+} \rangle$	0.472(16)	0.5	$\langle A_{z_2} A_{y_2^+} \rangle$	-0.515(15)	-0.5	$\langle A_{y_2^-} A_{h_2} \rangle$	0.470(15)	0.5
$\langle A_{y_2^-} \rangle$	0.515(15)	0.5	$\langle A_{z_2} A_{y_2^-} \rangle$	-0.472(16)	-0.5	$\langle A_{y_2^+} A_{h_3} \rangle$	0.510(15)	0.5
$\langle A_{y_3^+} \rangle$	0.491(15)	0.5	$\langle A_{z_3} A_{y_3^+} \rangle$	-0.500(15)	-0.5	$\langle A_{y_3^-} A_{y_3^+} \rangle$	-0.009(17)	0
$\langle A_{y_3^-} \rangle$	0.500(15)	0.5	$\langle A_{z_3} A_{y_3^-} \rangle$	-0.491(15)	-0.5	$\langle A_{y_3^-} A_{h_0} \rangle$	-0.810(10)	-0.833
$\langle A_{h_0} \rangle$	-0.279(16)	-0.333	$\langle A_{y_1^-} A_{y_1^+} \rangle$	-0.985(3)	-1	$\langle A_{y_3^+} A_{h_1} \rangle$	-0.814(10)	-0.833
$\langle A_{h_1} \rangle$	-0.322(17)	-0.333	$\langle A_{y_1^-} A_{h_0} \rangle$	-0.313(17)	-0.333	$\langle A_{y_3^+} A_{h_2} \rangle$	0.510(16)	0.5
$\langle A_{h_2} \rangle$	0.977(4)	1	$\langle A_{y_1^-} A_{h_1} \rangle$	-0.359(16)	-0.333	$\langle A_{y_3^-} A_{h_3} \rangle$	0.473(15)	0.5
$\langle A_{h_3} \rangle$	0.973(4)	1						
K-S Inequality (2)		$\sum_i \langle A_i \rangle - \frac{1}{4} \sum_{\langle i,j \rangle} \langle A_i A_j \rangle = 8.278 \pm 0.039$			K-S Inequality (3)		$\sum_{\alpha=0,1,2,3} \langle B_{h_\alpha} \rangle = 1.325 \pm 0.012$	

TABLE VI: The measured expectation values $\langle A_i \rangle$ and the correlations $\langle A_i A_j \rangle$ for all the compatible pairs under input states $|\Psi_5\rangle = (|0\rangle + |2\rangle)/\sqrt{2}$ and $|\Psi_6\rangle = (|1\rangle + |2\rangle)/\sqrt{2}$.

Input State $\rho_8 = \frac{1}{2}(0\rangle\langle 0 + 2\rangle\langle 2)$								
Observables	Experimental value	Theoretical prediction	Observables	Experimental value	Theoretical prediction	Observables	Experimental value	Theoretical prediction
$\langle A_{z_1} \rangle$	0.019(17)	0	$\langle A_{z_1} A_{z_2} \rangle$	0.014(17)	0	$\langle A_{y_1^+} A_{h_2} \rangle$	-0.151(17)	-0.167
$\langle A_{z_2} \rangle$	0.996(2)	1	$\langle A_{z_2} A_{z_3} \rangle$	-0.996(2)	-1	$\langle A_{y_1^+} A_{h_3} \rangle$	-0.166(16)	-0.167
$\langle A_{z_3} \rangle$	-0.014(17)	0	$\langle A_{z_1} A_{z_3} \rangle$	-0.019(17)	0	$\langle A_{y_2^-} A_{y_2^+} \rangle$	-0.997(1)	-1
$\langle A_{y_1^+} \rangle$	0.477(15)	0.5	$\langle A_{z_1} A_{y_1^+} \rangle$	-0.494(15)	-0.5	$\langle A_{y_2^-} A_{h_0} \rangle$	-0.611(19)	-0.667
$\langle A_{y_1^-} \rangle$	0.494(15)	0.5	$\langle A_{z_1} A_{y_1^-} \rangle$	-0.477(15)	-0.5	$\langle A_{y_2^+} A_{h_1} \rangle$	-0.630(17)	-0.667
$\langle A_{y_2^+} \rangle$	0.008(17)	0	$\langle A_{z_2} A_{y_2^+} \rangle$	0.005(17)	0	$\langle A_{y_2^-} A_{h_2} \rangle$	-0.666(17)	-0.667
$\langle A_{y_2^-} \rangle$	-0.005(17)	0	$\langle A_{z_2} A_{y_2^-} \rangle$	-0.008(17)	0	$\langle A_{y_2^+} A_{h_3} \rangle$	-0.647(18)	-0.667
$\langle A_{y_3^+} \rangle$	0.496(15)	0.5	$\langle A_{z_3} A_{y_3^+} \rangle$	-0.477(15)	-0.5	$\langle A_{y_3^-} A_{y_3^+} \rangle$	-0.027(17)	0
$\langle A_{y_3^-} \rangle$	0.477(15)	0.5	$\langle A_{z_3} A_{y_3^-} \rangle$	-0.496(15)	-0.5	$\langle A_{y_3^-} A_{h_0} \rangle$	-0.116(17)	-0.167
$\langle A_{h_0} \rangle$	0.367(17)	0.333	$\langle A_{y_1^+} A_{y_1^+} \rangle$	-0.030(17)	0	$\langle A_{y_3^+} A_{h_1} \rangle$	-0.135(16)	-0.167
$\langle A_{h_1} \rangle$	0.373(16)	0.333	$\langle A_{y_1^-} A_{h_0} \rangle$	-0.164(17)	-0.167	$\langle A_{y_3^+} A_{h_2} \rangle$	-0.124(17)	-0.167
$\langle A_{h_2} \rangle$	0.343(16)	0.333	$\langle A_{y_1^-} A_{h_1} \rangle$	-0.187(16)	-0.167	$\langle A_{y_3^-} A_{h_3} \rangle$	-0.177(17)	-0.167
$\langle A_{h_3} \rangle$	0.318(16)	0.333						
K-S Inequality (2)		$\sum_i \langle A_i \rangle - \frac{1}{4} \sum_{\langle i,j \rangle} \langle A_i A_j \rangle = 8.236 \pm 0.043$			K-S Inequality (3)		$\sum_{\alpha=0,1,2,3} \langle B_{h_\alpha} \rangle = 1.299 \pm 0.016$	

Input State $\rho_9 = \frac{1}{3}(0\rangle\langle 0 + 1\rangle\langle 1 + 2\rangle\langle 2)$								
Observables	Experimental value	Theoretical prediction	Observables	Experimental value	Theoretical prediction	Observables	Experimental value	Theoretical prediction
$\langle A_{z_1} \rangle$	0.316(19)	0.333	$\langle A_{z_1} A_{z_2} \rangle$	-0.333(18)	-0.333	$\langle A_{y_1^+} A_{h_2} \rangle$	-0.350(19)	-0.333
$\langle A_{z_2} \rangle$	0.352(17)	0.333	$\langle A_{z_2} A_{z_3} \rangle$	-0.352(17)	-0.333	$\langle A_{y_1^+} A_{h_3} \rangle$	-0.314(18)	-0.333
$\langle A_{z_3} \rangle$	0.333(18)	0.333	$\langle A_{z_1} A_{z_3} \rangle$	-0.316(19)	-0.333	$\langle A_{y_2^-} A_{y_2^+} \rangle$	-0.388(18)	-0.333
$\langle A_{y_1^+} \rangle$	0.333(18)	0.333	$\langle A_{z_1} A_{y_1^+} \rangle$	-0.304(18)	-0.333	$\langle A_{y_2^-} A_{h_0} \rangle$	-0.305(17)	-0.333
$\langle A_{y_1^-} \rangle$	0.304(18)	0.333	$\langle A_{z_1} A_{y_1^-} \rangle$	-0.333(18)	-0.333	$\langle A_{y_2^+} A_{h_1} \rangle$	-0.315(18)	-0.333
$\langle A_{y_2^+} \rangle$	0.309(18)	0.333	$\langle A_{z_2} A_{y_2^+} \rangle$	-0.303(19)	-0.333	$\langle A_{y_2^-} A_{h_2} \rangle$	-0.283(18)	-0.333
$\langle A_{y_2^-} \rangle$	0.303(18)	0.333	$\langle A_{z_2} A_{y_2^-} \rangle$	-0.309(18)	-0.333	$\langle A_{y_2^+} A_{h_3} \rangle$	-0.348(18)	-0.333
$\langle A_{y_3^+} \rangle$	0.356(19)	0.333	$\langle A_{z_3} A_{y_3^+} \rangle$	-0.337(18)	-0.333	$\langle A_{y_3^-} A_{y_3^+} \rangle$	-0.307(18)	-0.333
$\langle A_{y_3^-} \rangle$	0.337(18)	0.333	$\langle A_{z_3} A_{y_3^-} \rangle$	-0.356(18)	-0.333	$\langle A_{y_3^-} A_{h_0} \rangle$	-0.310(18)	-0.333
$\langle A_{h_0} \rangle$	0.365(18)	0.333	$\langle A_{y_1^+} A_{y_1^+} \rangle$	-0.363(19)	-0.333	$\langle A_{y_3^+} A_{h_1} \rangle$	-0.293(18)	-0.333
$\langle A_{h_1} \rangle$	0.355(18)	0.333	$\langle A_{y_1^-} A_{h_0} \rangle$	-0.355(17)	-0.333	$\langle A_{y_3^+} A_{h_2} \rangle$	-0.326(17)	-0.333
$\langle A_{h_2} \rangle$	0.281(18)	0.333	$\langle A_{y_1^-} A_{h_1} \rangle$	-0.357(18)	-0.333	$\langle A_{y_3^-} A_{h_3} \rangle$	-0.294(17)	-0.333
$\langle A_{h_3} \rangle$	0.383(17)	0.333						
K-S Inequality (2)		$\sum_i \langle A_i \rangle - \frac{1}{4} \sum_{\langle i,j \rangle} \langle A_i A_j \rangle = 8.248 \pm 0.050$			K-S Inequality (3)		$\sum_{\alpha=0,1,2,3} \langle B_{h_\alpha} \rangle = 1.309 \pm 0.018$	

TABLE VII: The measured expectation values $\langle A_i \rangle$ and the correlations $\langle A_i A_j \rangle$ for all the compatible pairs under input states $\rho_8 = (|0\rangle\langle 0| + |2\rangle\langle 2|)/2$ and $\rho_9 = (|0\rangle\langle 0| + |1\rangle\langle 1| + |2\rangle\langle 2|)/3$.